



2D Ising Model With Point Defect at Adjacent Sites

Sagar Kanwar, Sudeep Lamichhane, Pankaj Singh Dhami, and Narayan Adhikari^{*)}

Central Department of Physics, Tribhuvan University, Kathmandu, Nepal

Abstract. The study examines the magnetization behaviour in a 2D Ising model with single and double point defects using Monte Carlo simulations. At elevated temperatures, thermal fluctuations dominate, leading to a disordered state with negligible magnetic moment. As temperature decreases, defects influence spin alignment. At very low temperatures, the magnetization due to single-point defects is minimal, whereas two-point defects significantly alter magnetization. This occurs due to local perturbations in spin alignment, leading to disruptions in nearby spins and reducing overall magnetization. Additionally, thermal fluctuations play a crucial role in the behavior of the Ising model at finite temperatures. Point defects can increase thermal fluctuations around the defect sites, further contributing to the reduction in overall magnetization. The findings presented in this research contribute to a better understanding of the role of defects in magnetic systems, with potential applications in material science. Further investigations using larger lattice sizes and higher defect concentrations could provide more insights in optimizing magnetic properties in real-world systems.

Submitted: November 2, 2024;

Revised: May 30, 2024;

Accepted: June 1, 2025

Keywords: Acceptance Ratio; Heat Capacity; Ising Model; Magnetization; Susceptibility

INTRODUCTION

The Ising model [1], also known as the Lenz-Ising model, named after physicists Ernst Ising and Wilhelm Lenz, is a mathematical model that is used to study phase transitions in statistical mechanics. In this model, all the atoms are supposed to be at a lattice site. Each atom is considered a magnetic dipole. Each dipole can have one of the two possible states, i.e., either spin up ($s = +1$) or spin down ($s = -1$) [2]. And only the nearest neighbour attraction between the dipoles is taken into account [1, 2]. Neighboring spins that agree have lower energy than those that disagree. The system tries to attend to the lowest energy state, but heat disturbs this tendency, and the system has different states. The 2D Ising model is the simplest statistical model to show phase transition [3, 4]. The one-dimensional Ising model was solved by Ising alone in his thesis in 1925 and found that it shows no phase transition. 2D Ising is much harder to solve analytically and was given much later by Lars Onsager in 1944 [5]. This model is often used to study phase transitions, such as transitions between paramagnetic and ferromagnetic states [6].

No crystal in nature is perfect; defects always exist within the structure. In crystallography, a point defect refers to

a type of imperfection that occurs at a single lattice point within a crystal structure. These defects [7] can arise due to various reasons, such as thermal vibration, impurities, or other external factors [6].

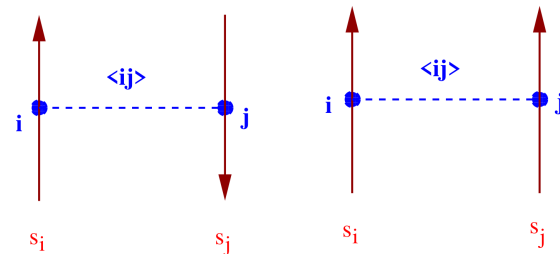


FIGURE 1: Schematic representation: nearest neighbour spins facing opposite direction (left) and facing same direction (right) [8].

Point defects can have a significant impact on the physical, chemical, and electrical properties of materials [10]. There are several types of point defects in crystals. Some of them are:

- **Vacancy Defect** - This type of defect exists in crystal due to the absence of basis at the lattice site. The defect moves to the opposite site with the movement of a neighbouring atom as it moves to occupy a vacant site.

^{*)}Corresponding author: narayan.adhikari@cdp.tu.edu.np

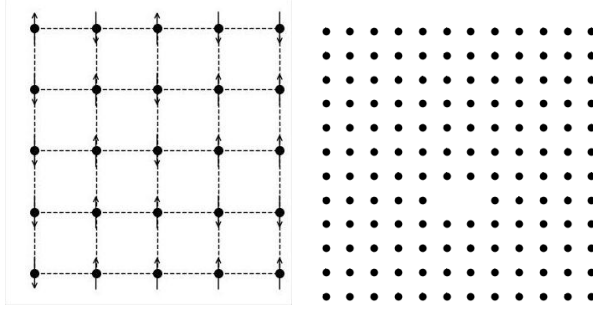


FIGURE 2: Orientation of atomic spin, where spin can take only two values, either spin up or down (left), and a 2D square lattice with two point defects at positions 78 and 79, counted from the top-left corner in a row-major order (right) [9].

- **Frenkel Defect** - This type of point defect arises due to the movement of a normal atom at the lattice site to the interstitial region [11].
- **Schottky defect** - Vacancy created by the movement of atoms from the interior of the crystal to the surface [12, 13].
- **Interstitial** - An interstitial defect occurs when an atom occupies a site within the crystal that is normally empty. This results in an extra atom squeezed between the regular lattice positions.

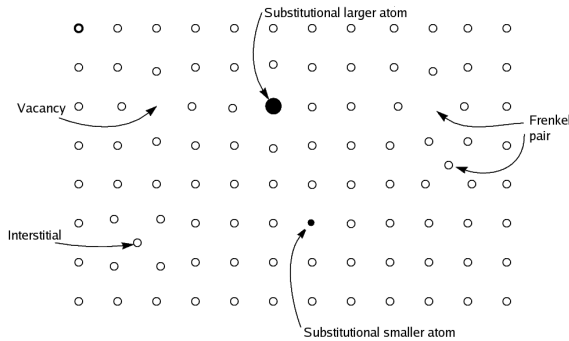


FIGURE 3: Schematic diagram showing some point defects.

Point defects play a significant role in altering a wide range of material properties, including electrical conductivity, optical characteristics, mechanical strength, and diffusion rates [14, 15]. Understanding and controlling these defects are essential in diverse fields like material science, solid-state physics, and chemistry, as they allow for the manipulation and comprehension of material behavior [16, 17].

METHODOLOGY

In this study, the Ising model with point defects is analyzed using computational methods. The system is simulated using the Monte Carlo method on square lattices with dimensions 12×12 , 20×20 and 25×25 . Single and two-point defects are introduced to study their effect on specific heat capacity, susceptibility, and magnetization. The obtained results are approximate, yet they hold significant importance from a physics perspective since they represent the simplest and phenomenologically interesting model of a ferromagnetic material.

Monte Carlo Simulation

Monte Carlo simulations are performed using the Metropolis algorithm, which updates the spin configuration iteratively as follows:

1. Select a random spin s_i from the lattice.
2. Compute the energy change ΔE due to a proposed spin flip ($s_i \rightarrow -s_i$):

$$\Delta E = 2J s_i \sum_j s_j, \quad (1)$$

where the summation runs over the nearest neighbors of s_i .

3. Accept the spin flip with probability:

$$P = \begin{cases} e^{-\beta \Delta E}, & \text{if } \Delta E > 0, \\ 1, & \text{if } \Delta E \leq 0. \end{cases} \quad (2)$$

Here, $\beta = 1/k_B T$ is the inverse temperature, where k_B is set to 1 for simplicity.

Each simulation begins with a random spin configuration and is evolved for 10^6 Monte Carlo steps per site (MCS) to reach thermal equilibrium. Observables are then averaged over an additional 10^6 MCS.

THEORETICAL BACKGROUND

The Ising Model

The Hamiltonian of Ising model is [1]

$$H(\{s_i\}) = - \sum_{\langle i, j \rangle} J_{ij} s_i s_j - B \sum_i s_i$$

The sum $\langle i, j \rangle$ is over nearest neighbors ($j = i \pm 1$ in 1D).

where:

- H : Hamiltonian
- $\langle i, j \rangle$: nearest neighbor interaction
- J_{ij} : interaction energy between spins i and j
- S_i : spin of site i
- S_j : spin of site j
- B : external magnetic field

Consider a square lattice with N lattice sites, i.e., $i = 1, 2, 3, \dots, N$. In this, each site has four nearest neighbours with which it can interact. The Hamiltonian of the isotropic system will be

$$H = -J \sum_{\langle i, j \rangle} S_i S_j - B \sum_{i=1}^N S_i \quad (3)$$

Here, J represents strength of isotropic spin, B represents external field and S_i, S_j represents spin of i^{th} and j^{th} site. If $J > 0$, then the system is ferromagnetic and $J < 0$, paramagnetic [18].

At zero magnetic field, the system undergoes 2^{nd} order phase transition from ordered state to disordered state at a critical value, β_c , where

$$\beta_c = \frac{1}{2} \ln(1 + \sqrt{2}) \approx 0.44068 \dots \quad (4)$$

Here, magnetization acts as an order parameter.

The acceptance ratio, $A(\mu \rightarrow \nu)$ which is the probability of state ν being selected when the system is in state μ is given by [8]

$$A(\mu \rightarrow \nu) = \begin{cases} \exp(-\beta(E_\nu - E_\mu)) & \text{if } E_\nu - E_\mu \geq 0, \\ 1 & \text{if } E_\nu - E_\mu \leq 0. \end{cases} \quad (5)$$

Implementation

The selection of the initial configuration can play a vital role in determining the thermalization speed or potentially impeding it entirely. While the model under investigation may downplay its importance, we will acknowledge its relevance in studying other systems. We have two options: a “cold” initial configuration or a “hot” configuration. It is advisable to begin with one of these states on large lattices and then gradually adjust the temperature in small increments. After each temperature change, the spin configuration is saved and used in the subsequent simulation. Consider that initially the system is in the state $\mu = \{S_1^\mu, \dots, S_k^\mu, \dots, S_N^\mu\}$ and after transition it goes to the state $\nu = \{S_1^\nu, \dots, S_k^\nu, \dots, S_N^\nu\}$, differing only by single spin. Here each step in the Markov process is determined by the Metropolis algorithm. Then change in energy is

$$E_\nu - E_\mu = 2S_k^\mu \left(\sum_{\langle ij \rangle} S_i^\mu \right) \quad (6)$$

Where $S_k^\nu - S_k^\mu = -2S_k^\mu$. In this new state, a transition is considered valid if it reduces the energy of the system and a spin flip occurs. If it increases the energy, then we evaluate the acceptance ratio using the formula $A(\mu \rightarrow \nu) = \exp(-\beta(E_\nu - E_\mu))$, where E_μ and E_ν represent the initial and final energies, respectively, and β is a constant related to temperature. When this acceptance ratio is less than one, the spin flip is accepted. To perform the spin flip, we incorporate the concept of a random number, which is uniformly distributed in the range $0 \leq x < 1$. If this random number x is less than or equal to the acceptance ratio $A(\mu \rightarrow \nu)$, the change is accepted. On the other hand, if x is greater than $A(\mu \rightarrow \nu)$, the change is rejected. This approach allows for the exploration of different states while ensuring that the system evolves towards lower energy configurations.

The value of energy is calculated by using

$$E = - \sum_{\langle ij \rangle} S_i S_j, \quad (7)$$

And the value of magnetization is calculated by using

$$M = \left| \sum_i S_i \right|. \quad (8)$$

Here we use normalized value

$$\langle e \rangle = \frac{1}{2N} \langle E \rangle, \quad \text{and} \quad \langle m \rangle = \frac{1}{N} \langle M \rangle \quad (9)$$

The specific heat can be evaluated using

$$c = \beta^2 N (\langle (e - \langle e \rangle)^2 \rangle) = \beta^2 N (\langle e^2 \rangle - \langle e \rangle^2) \quad (10)$$

and the magnetic susceptibility can be evaluated using the relation

$$\chi = \beta N (\langle (m - \langle m \rangle)^2 \rangle) = \beta N (\langle m^2 \rangle - \langle m \rangle^2) \quad (11)$$

To estimate the data requirement for precise measurements of these quantities, we take into account that as the number of independent measurements (nn) increases, the statistical error decreases approximately at a rate of $1/\sqrt{n}$ [8].

RESULTS AND DISCUSSIONS

For square lattice with dimension $L=12$.

• Heat Capacity (C_v)

From Figure 4, we can see the introduction of single point defect, the transition temperature shifts towards left ($\beta = 0.42$) and the heat capacity decreases ($C_v = 174.254$). For a two-point defect, the transition temperature shifts right ($\beta = 0.445$) and the value of heat capacity also decreases ($C_v = 165.706$).

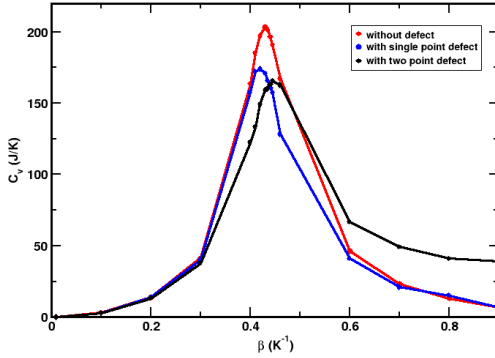


FIGURE 4: Heat capacity C_v vs. β for a 12×12 lattice. The presence of point defects decreases the C_v values, with a greater reduction observed for two point defects compared to a single point defect. The transition temperature shifts left for a single defect and right for two defects.

• Susceptibility (χ)

The point of phase transition does not change for lattices without defects and with single-point defects. But the value of susceptibility decreases to 2.412×10^{-2} (single point defect) from 2.498×10^{-2} (without defect). For a two-point defect, the point of phase transition shifts towards the right ($\beta = 0.42$) and the value of susceptibility decreases to 2.249×10^{-2} .

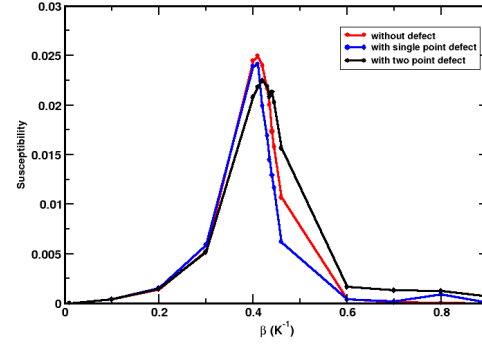


FIGURE 5: Susceptibility χ vs. β for a 12×12 lattice. Point defects reduce χ , with two defects causing a greater decrease. The transition point shifts slightly for two defects but remains nearly unchanged for a single defect.

• Magnetization (M)

Figure 6 illustrates the magnetization versus β plots for a square lattice without defects, with a single point defect at position 78 and with two point defects at positions 78 and 79. The simulations span the β range from 0.01 to 0.9. Below the transition temperature, all three graphs exhibit a similar starting point. However, above the transition temperature (at $\beta = 0.9$), the magnetization values differ slightly. Without any defects, the magnetization is 0.998; with a single point defect, it is 0.998; and with two point defects, it reduces to 0.949.

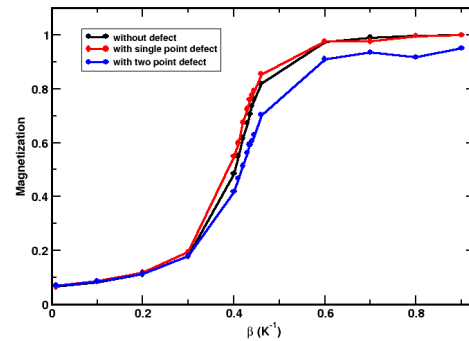


FIGURE 6: Magnetization M vs. β for a 12×12 lattice. Point defects disrupt spin alignment, leading to reduced magnetization, with a stronger effect observed for two-point defects. Above the transition temperature, defects cause a slight reduction in M , with two defects having a more pronounced effect.

For square lattice with dimension $L = 20$.

• **Heat Capacity (C_V)**

The values of beta are 0.435, 0.43, and 0.44 for lattices without defects, with single point defects, and with two point defects, respectively. And the value of heat capacity for lattice without defect is 664.808, with a single point defect is 632.261, and with a two-point defect is 602.845.

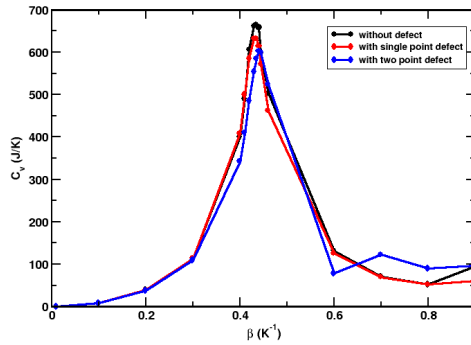


FIGURE 7: Heat capacity C_V vs. β plot for a 20×20 lattice. Compared to $L = 12$, the peak of C_V increases, indicating a sharper phase transition. Point defects still lower C_V , with a more noticeable reduction in larger lattices.

• **Susceptibility (χ)**

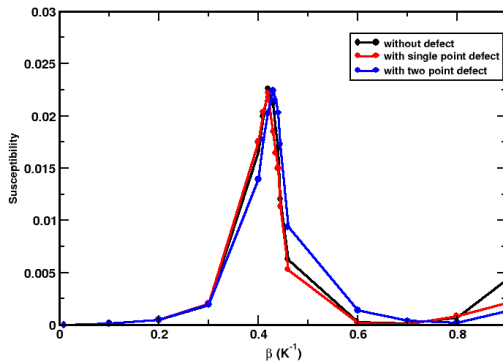


FIGURE 8: Susceptibility χ vs. β for a 20×20 lattice. The peak is higher and sharper than in $L = 12$, reflecting a more pronounced phase transition. Defects still suppress χ , though their effect diminishes slightly as L increases.

The phase transition for square lattice without defect and with single point defect takes place at $\beta = 0.42$ and the value of susceptibility to be $2.258 \times$

10^{-2} and 2.217×10^{-2} . For a lattice with two-point defect, the phase transition takes place at $\beta = 0.43$ and the corresponding value of susceptibility to be 2.241×10^{-2} .

• **Magnetization (M)**

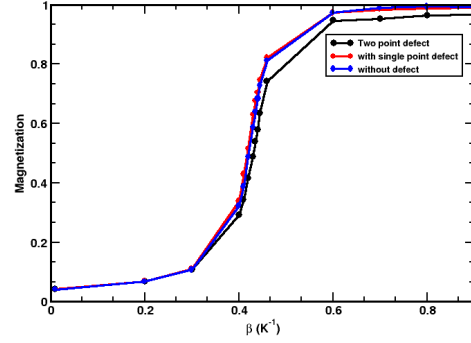


FIGURE 9: Magnetization M vs. β for a 20×20 lattice. The transition appears sharper compared to $L = 12$. Defects still lower M , especially above the transition point. The presence of point defects lowers magnetization, especially for two point defects.

In Figure 9, we present the magnetization versus β plots for a square lattice with dimension $L = 20$ without defects, with a single point defect at site 78, and with two point defects at sites 78 and 79. Notably, below the transition temperature, all three graphs exhibit identical starting points. However, as the temperature crosses the transition threshold, particularly at $\beta = 0.9$, the magnetization values begin to diverge. For the square lattice without defects, the magnetization at $\beta = 0.9$ is 0.992. In the presence of a single-point defect at site 78, the magnetization is slightly reduced to 0.989. Furthermore, with two point defects at sites 78 and 79, the magnetization is notably lower, measuring 0.967 at $\beta = 0.9$. These results highlight the significant impact that point defects can have on the magnetization behavior of the 2D Ising model, particularly as the system approaches and surpasses the critical temperature.

For square lattice with dimension $L=25$

• **Heat Capacity (C_v)**

For a square lattice without defect, with a single point defect, the transition point remains the same ($\beta = 0.435$) and for a two-point defect, it is $\beta = 0.445$. The values of heat capacity for lattices without defects, with single-point defects, and with two-point defects are 1122.249, 1064.203, and 1037.384.

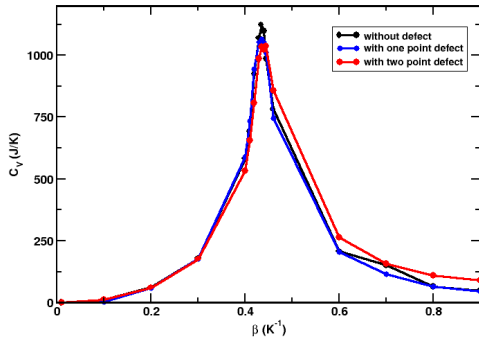


FIGURE 10: Heat capacity C_v vs. β for a 25×25 lattice. The peak continues to rise with increasing L , showing stronger phase transition behavior. Defects reduce C_v , though their relative impact lessens as the lattice size grows.

• **Susceptibility (χ)**

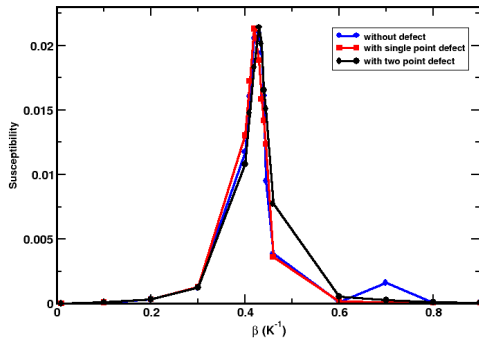


FIGURE 11: Susceptibility χ vs. β plot for a 25×25 lattice. Compared to $L = 20$, the peak continues to rise. The reduction due to defects remains present, but their relative influence weakens as the system size grows.

The phase transition point for lattice without defect is $\beta = 0.43$ and the value of susceptibility

is 2.097×10^{-2} . For a square lattice with a single point defect, the value of phase transition is $\beta = 0.42$ and the value of susceptibility is 2.131×10^{-2} . And for two-point defects, $\beta = 0.43$ and $\chi = 2.141 \times 10^{-2}$.

• **Magnetization (M)**

Figure 12 showcases the magnetization versus β plots for a square lattice with dimension $L = 25$, representing the behavior without defects, with a single point defect at site 78, and with two point defects at sites 78 and 79. It is intriguing to observe that all three graphs emanate from a common point at $\beta = 0.01$, demonstrating the alignment of initial magnetization values. As the temperature rises and surpasses the critical point, particularly at $\beta = 0.9$, distinctive trends emerge in the magnetization values. For the square lattice without defects, the magnetization reaches 0.998 at $\beta = 0.9$. In the presence of a single-point defect at site 78, the magnetization slightly decreases to 0.995. Furthermore, with two point defects at sites 78 and 79, the magnetization is further reduced, measuring 0.979 at $\beta = 0.9$.

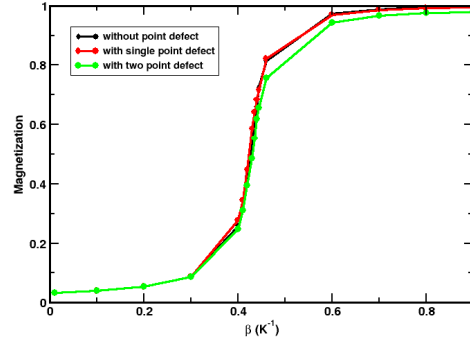


FIGURE 12: Magnetization M vs. β for a 25×25 lattice. The transition further sharpens with increasing $L = 25$. The impact of defects remains significant, though their relative influence decreases as lattice size increases.

From the data, it is clear that the value of magnetization is slightly different at high temperatures. This is because at high temperatures the system is in a disordered state and most of the spin cancels each other, but there exists a negligible amount of magnetic moment. As we start to decrease temperature, the defects start to play a role. At very low temperatures, there is almost no difference in magnetization without and with a single-point defect. But a two-point defect brings considerable change in magnetic moment. The point defect causes a local perturbation in

the lattice's spin alignment. Nearby spins will experience a disruption in their alignment due to the defect, leading to a slight decrease in the overall magnetization of the lattice.

Another probable reason for the decrease in magnetization is thermal fluctuation. At finite temperatures, thermal fluctuations play a significant role in the behavior of the Ising model. The introduction of a point defect can lead to an increase in thermal fluctuations around the defect site, which can further reduce the overall magnetization of the lattice. The marked influence of two-point defects on magnetization underscores the significance of defect configurations. We hope that our findings will inspire further investigations into more complex systems and pave the way for innovative approaches in materials science, advancing our understanding of magnetic materials and their potential applications.

CONCLUSION AND OUTLOOKS

In this study, we have meticulously investigated the 2D Ising model by performing extensive simulations for a range of β values from 0.01 to 0.9. By examining the magnetization with and without point defects at each β value, intriguing insights have been uncovered. Our results reveal that the presence of a single point defect has only a marginal effect on the magnetization of the system. Contrarily, the introduction of two-point defects brings about a substantial change in the magnetization behavior. This observation highlights the distinct impact that different defect configurations can exert on the Ising model. The underlying reasons for these contrasting effects lie in the intricate interplay between the lattice's spin alignment and thermal fluctuations. The single-point defect appears to cause local perturbations in the spin alignment, leading to minimal changes in magnetization. On the other hand, the two-point defects disrupt nearby spins more significantly, resulting in a pronounced alteration in the overall magnetization of the lattice.

The 2D Ising model has been expertly explored using the powerful Markov Chain Monte Carlo method, and fascinating insights have been uncovered through simulations on square lattices of dimensions 12, 20, and 25. The introduction of single and double point defects has indeed induced subtle changes in magnetization. However, to fully unravel the profound impact of defects on the Ising model, it is highly recommended to expand our investigations to larger lattice dimensions. Embracing the allure of more point defects in the system promises to unveil captivating new facets of the model's behavior. Venturing into the realm of larger lattice sizes offers an exciting avenue for future research. By delving into extensive lattice dimensions, we can unlock previously unseen nuances of the Ising model with point defects. The allure of

unexplored possibilities awaits, revealing how these defects intertwine with the intricate magnetic interactions on a grander scale.

CONFLICT OF INTEREST

The authors declare that there is no conflict of interest regarding the publication of this paper.

REFERENCES

1. B. A. Cipra, "An introduction to the ising model," *The American Mathematical Monthly*, vol. 94, no. 10, pp. 937–959, 1987.
2. E. Ising, "Beitrag zur theorie des ferromagnetismus," *Zeitschrift für Physik*, vol. 31, pp. 253–258, 1925.
3. B. McCoy and T. Wu, *The Two-Dimensional Ising Model: Second Edition*. Dover books on physics, Dover Publications, 2014.
4. B. M. McCoy and T. T. Wu, *The two-dimensional Ising model*. Harvard University Press, 1973.
5. L. Onsager, "Crystal statistics. i. a two-dimensional model with an order-disorder transition," *Physical Review*, vol. 65, no. 3-4, p. 117, 1944.
6. V. S. Dotsenko and V. S. Dotsenko, "Critical behaviour of the phase transition in the 2d ising model with impurities," *Advances in Physics*, vol. 32, no. 2, pp. 129–172, 1983.
7. A. B. Harris, "Effect of random defects on the critical behaviour of ising models," *Journal of Physics C: Solid State Physics*, vol. 7, no. 9, p. 1671, 1974.
8. K. N. Anagnostopoulos, *A Practical Introduction to Computational Physics and Scientific Computing*. 1st ed., 2014.
9. C. Kittel, "Introduction to solid state physics eighth edition," 2021.
10. O. Madelung, *Introduction to Solid-State Theory*. Springer Series in Solid-State Sciences, Springer, 1996.
11. J. Frenkel, "Zur theorie der elastizitätsgrenze und der festigkeit," *Zeitschrift für Physik*, vol. 35, p. 652, 1926.
12. C. Wagner and W. Schottky, "Zur theorie der oxidation von metallen," *Zeitschrift für physikalische Chemie*, vol. 163, 1931.
13. W. Schottky, "Zur theorie der elektrolyte," *Zeitschrift für physikalische Chemie*, vol. B29, p. 353, 1935.
14. P. Peterson, E. Baker, and B. McGaw, eds., *International Encyclopedia of Education*. 3rd ed., April 17 2009.
15. D. Hubbard and D. A. Samuelson, "Modeling without measurements," *OR/MS Today*, pp. 28–33, October 2009.
16. N. Metropolis, A. W. Rosenbluth, M. N. Rosenbluth, A. H. Teller, and E. Teller, "Equation of state calculations by fast computing machines," *The journal of chemical physics*, vol. 21, no. 6, pp. 1087–1092, 1953.
17. W. K. Hastings, "Monte carlo sampling methods using markov chains and their applications," 1970.
18. A. J. Dekker, "Ferromagnetism, antiferromagnetism, and ferrimagnetism," in *Solid State Physics*, pp. 464–497, Springer, 1981.